Supplementary Information

Michael P. Mercer, Arihant Bhandari, Chao Peng,
Jacek Dziedzic, Chris K. Skylaris, and Denis Kramer

1 Nanoparticle geometry in electrolyte

Relaxed geometries of H-terminated and O-terminated nanoparticles in electrolyte are presented in Figure S1a and Figure S1b, respectively.

2 Nanoparticle geometry dependent on particle size

Relaxed geometries of H-terminated nanoparticles of variable particle size are presented in Figure S2.

3 Directional dependence of the potential and charge density

As shown by the Mulliken analysis in the main paper, the O-terminated nanoparticles show some dependence of the atomic charge partitioning on the direction around the particle. Also, this directional dependency is a function of the environment, either vacuum or electrolyte. To explore this behaviour in further detail, the potential distribution is shown around the nanoparticle in vacuum in Figure S3. The potential distribution as well as the charge density in electrolyte are shown in Figure S4. The figures reveal that the potential and charge density around the particle closely follow the distribution of the charges near the edge atoms determined from Mulliken analysis. In vacuum, some of the peroxide (O-O) bonds on the edge are broken, whereas in electrolyte, these bonds remain preserved around the nanoparticle, as best exemplified in Figure S4c and Figure S4f. The electrolyte results show close to zero potential around the six edges and a strongly negative potential (and hence positive electrolyte counter-charge) in the vicinity of the corners. The reasons for the different bonding arrangement in electrolyte compared with vacuum are not fully understood and will be resolved in future work after further method development.

4 Averaging of potential to determine the work function

As mentioned in the paper, the work function can be determined from

$$\psi(r) = -e\phi(r) - E_{\mathrm{F}}, \tag{S1}$$

where the terms were as defined in the main paper.

In principle, it is expected that $\phi(r)$ becomes constant as $r \to \infty$ and that $\psi(r \to \infty)$ is equivalent to the work function. It wasn't practical, however, to compute the potential for an infinitely-sized

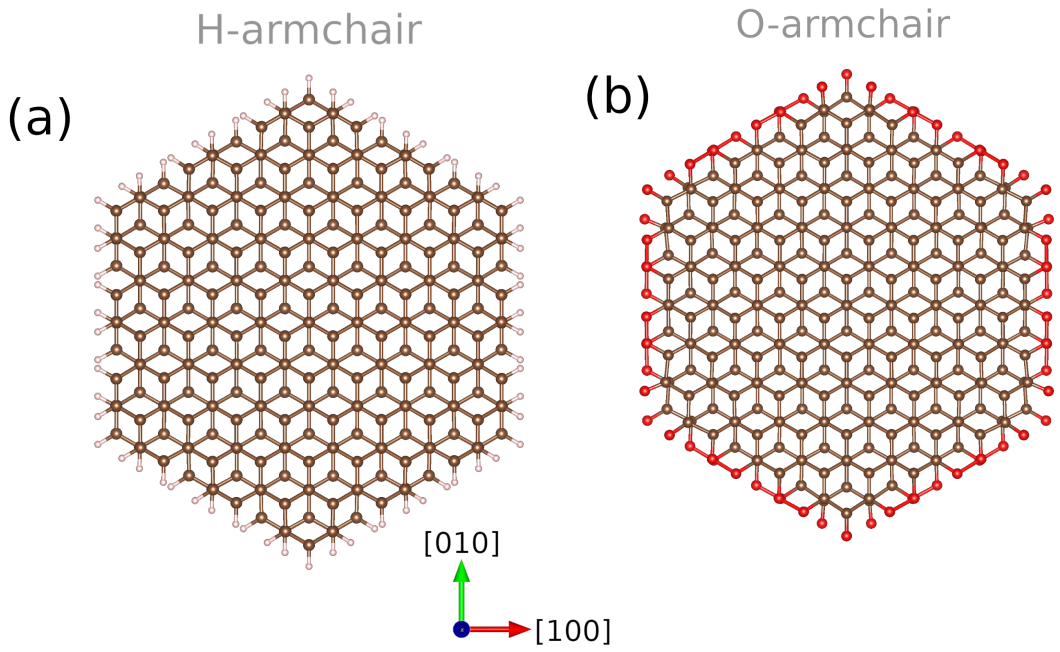

Fig. S1: Relaxed geometries, in electrolyte, of graphite nanoparticles terminated by (a) H or (b) O.

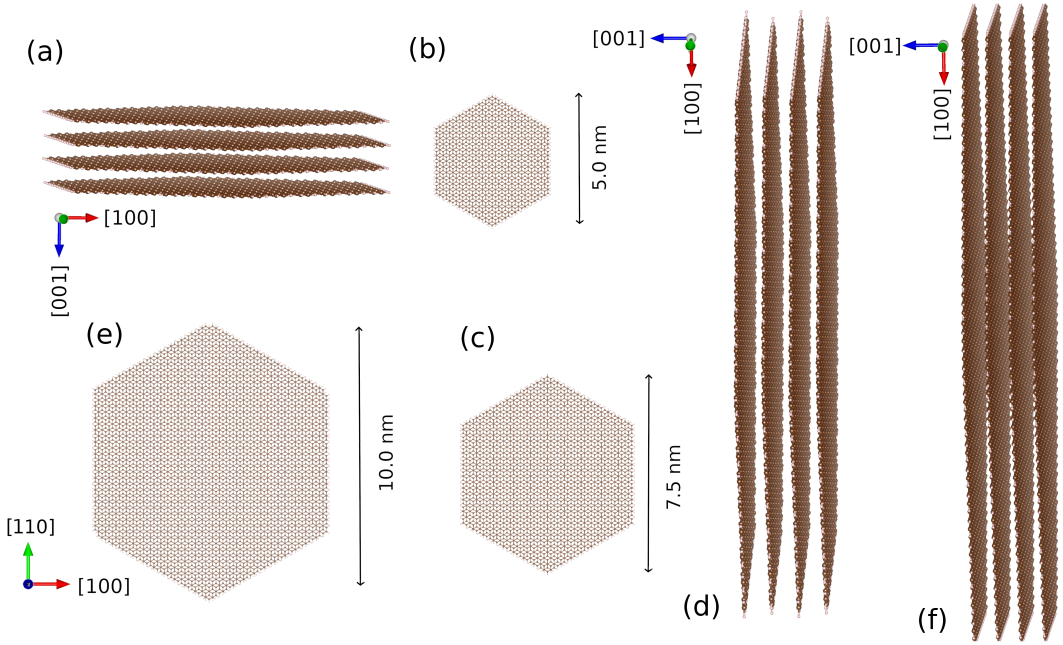

Fig. S2: Relaxed geometries, in vacuum, of graphite nanoparticles terminated by H. The number of atoms in total was (a,b); 2800 atoms; (c,d): 5600 atoms; (e,f): 10148 atoms.

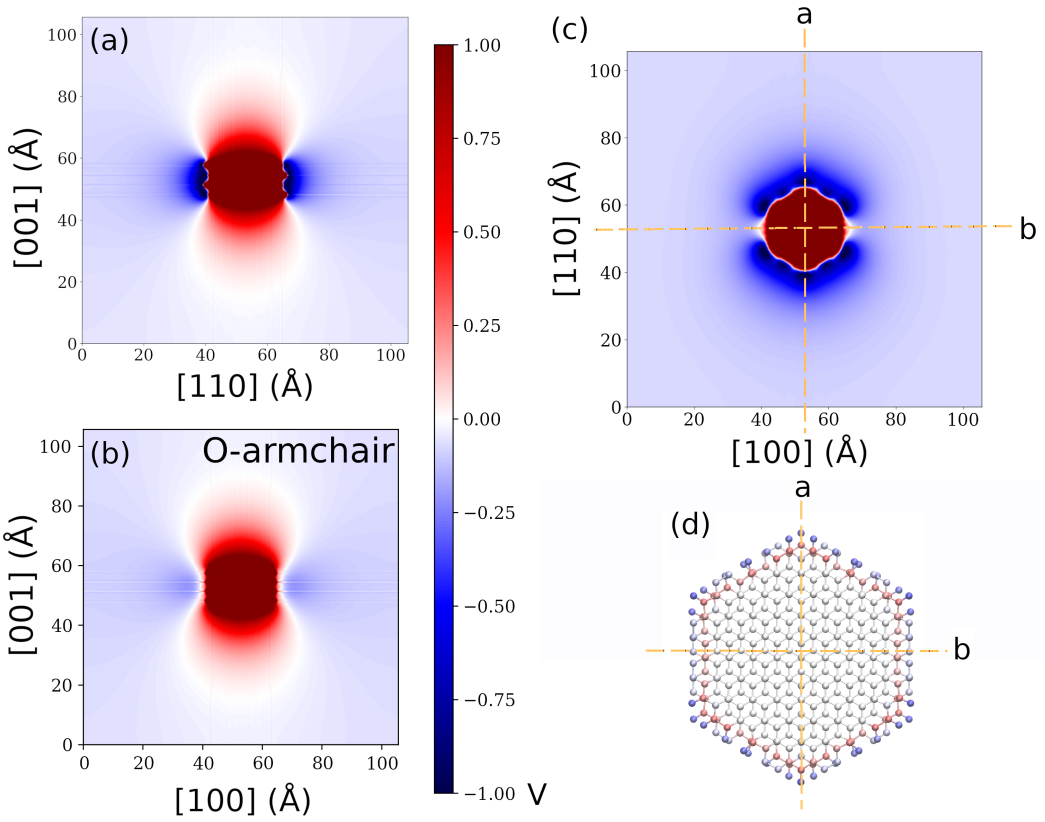

Fig. S3: Potential distribution around the O-terminated nanoparticle in vacuum. Results are shown (a) in the [001]-[110] plane, (b) in the [001]-[100] plane as presented in the main paper (c) in the [110]-[100] plane. All planes intersect the mid-point of the simulation cell. In (c), the dashed lines indicate the two perpendicular planes through which cross sections (a) and (b) are taken. Also shown is the Mulliken analysis of the particle, also showing the directions through which the cross sections are taken.

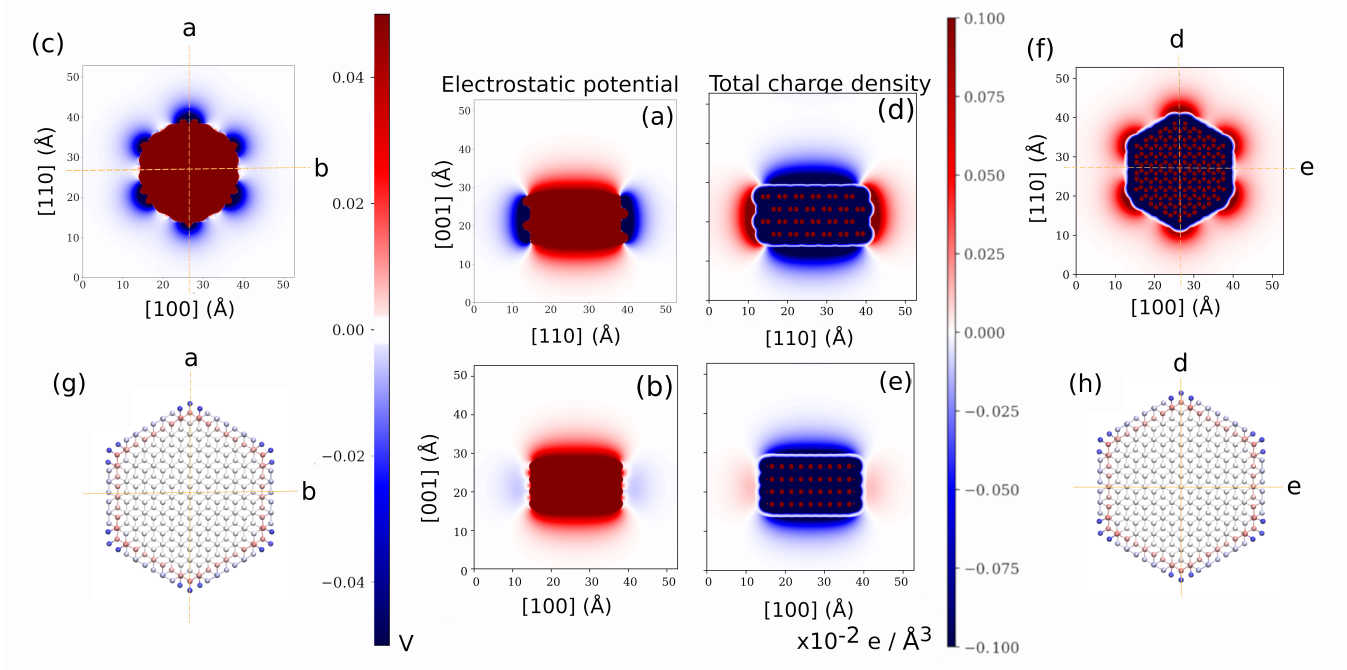

Fig. S4: (a-c): Potential distribution around the O-terminated nanoparticle in electrolyte. Results are shown (a) in the [001]-[110] plane, (b) in the [001]-[100] plane as presented in the main paper (c) in the [110]-[100] plane. All planes intersect the mid-point of the simulation cell. In (c), the dashed lines indicate the two perpendicular planes through which cross sections (a) and (b) are taken. (d-f): Total charge density around the O-terminated nanoparticle in electrolyte. Results are shown (d) in the [001]-[110] plane, (e) in the [001]-[100] plane as presented in the main paper (f) in the [110]-[100] plane. All planes intersect the mid-point of the simulation cell. In (f), the dashed lines indicate the two perpendicular planes through which cross sections (d) and (e) are taken. Also shown in (g-h) is the Mulliken analysis of the particle in electrolyte, also showing the directions through which the cross sections are taken.

simulation cell. To estimate the potential at the cell boundary of a finite-sized cell, an average value of ϕ was taken at the points A and B indicated in Figure S5. The work function ψ was determined from

$$\psi \approx -e\left(\frac{\phi_A + \phi_B}{2}\right) - E_{\mathrm{F}} = -e\phi_{\mathrm{avg}} - E_{\mathrm{F}}, \tag{S2}$$

where ϕ_A and ϕ_B were the potentials at points A and B, respectively, along the cell boundary, and ϕ_{avg} represents the average potential from these two points.

To test the robustness of the values computed using equation S2, results were compared with two simulation cell sizes shown in Figure S5a and Figure S5b, computed for each of the four nanoparticle sizes shown in the main paper. As shown in Figure S5c, results are insensitive to the size of the simulation cell, with the difference between the work function computed with both simulation cell sizes being less than 0.02 eV for all nanoparticle sizes.

5 Table of all work function values

The work functions of all the systems examined in the work, in vacuum, are shown in Table S1.

Table S1: Work function (ψ) obtained for different systems, in vacuum. For the nanoparticle systems, the particle size along the [110]-direction is also presented.

System	Work function ψ (eV)	Size (nm)
Basal plane	4.15	-
Planar edge (H-armchair)	2.89	-
Nanoparticle (H-armchair)	3.51	2.5
	3.66	5.0
	3.75	7.5
	3.85	10.0
Planar edge (O-armchair)	5.26	-
Nanoparticle (O-armchair)	6.26	2.5

6 Determination of work function in electrolyte

Calculations in vacuum were performed with pseudo ions, but those in electrolyte were performed with smeared ions to enable solution of the Poisson-Boltzmann equation. It was found for the basal plane systems in the main text that the calculated work function values in electrolyte were shifted by a constant value with respect to those in vacuum, due to the lower potential oscillations near the atomic cores with smeared ions.

We can estimate the error introduced by the implementation of smeared ions in the electrolyte model from Figure S6- S8. As we decrease the smearing width, σ, of the smeared ions, the electrostatic potential becomes steeper. In the limit of σ approaching the width of the pseudopotential cores, the work function due to smeared ions approach the same values as the ones resulting from pseudopotentials. Comparing the calculations in vacuum (solid lines) with those in electrolyte (dashed lines), the electrolyte effect on the work function values is small. Quantitatively, the electrolyte lowers the work functions by -0.0835 eV compared with vacuum.

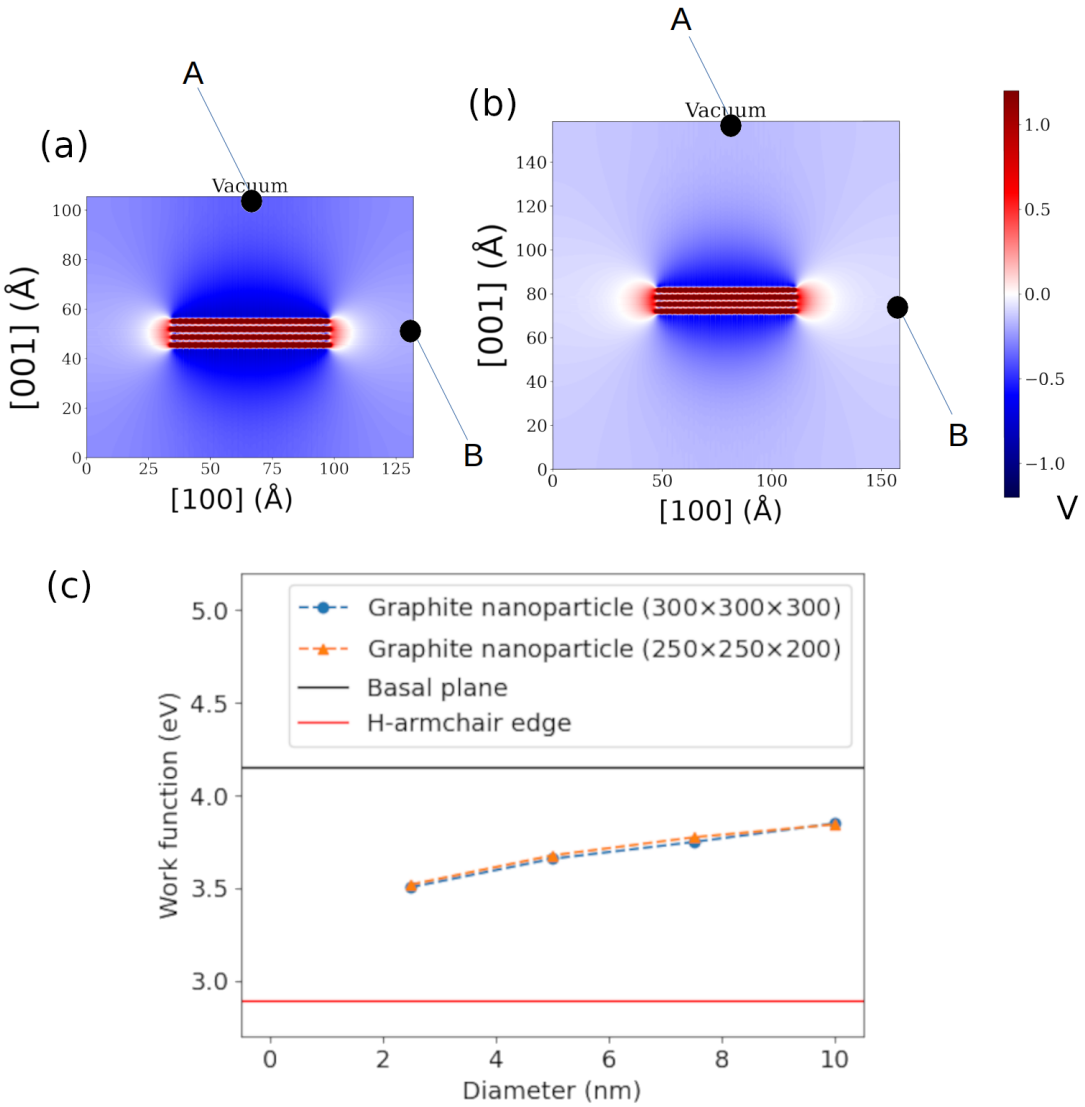

Fig. S5: Scheme to illustrate how the average potential around the nanoparticle was estimated dependent on the cell size. An example is illustrated with the H-armchair graphite nanoparticle consisting of 5600 atoms. A cross section of the potential was taken using the method described in the main paper. The potential was computed within (a) a 250×250×200 Bohr^3 cell; (b) a 300×300×300 Bohr^3 cell. In both cases, the potential ϕ was determined at the mid-point of the [100]-direction at the top of the presented cross-section (point A) and the mid-point of the [001]-direction on the right hand side (point B). The average of ϕ at points A and B was taken to estimate the value of ϕ at the cell boundary. This was done for each of the 4 nanoparticle sizes shown in (c) and the main paper. The work function determined for the two cell sizes is shown as a function of particle size in (c).

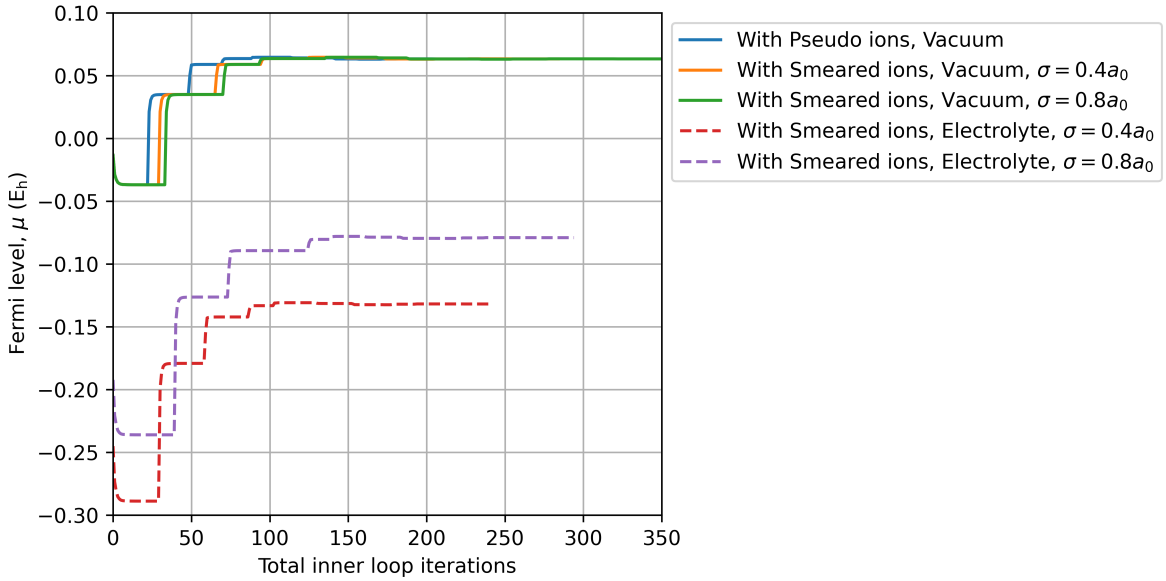

Fig. S6: Evolution of the Fermi level, μ, of the system with total inner loop iterations. a_0 is the Bohr radius. Results are shown for pseudo ions, and for smeared ions with variable smearing width, σ (as indicated in the legend).

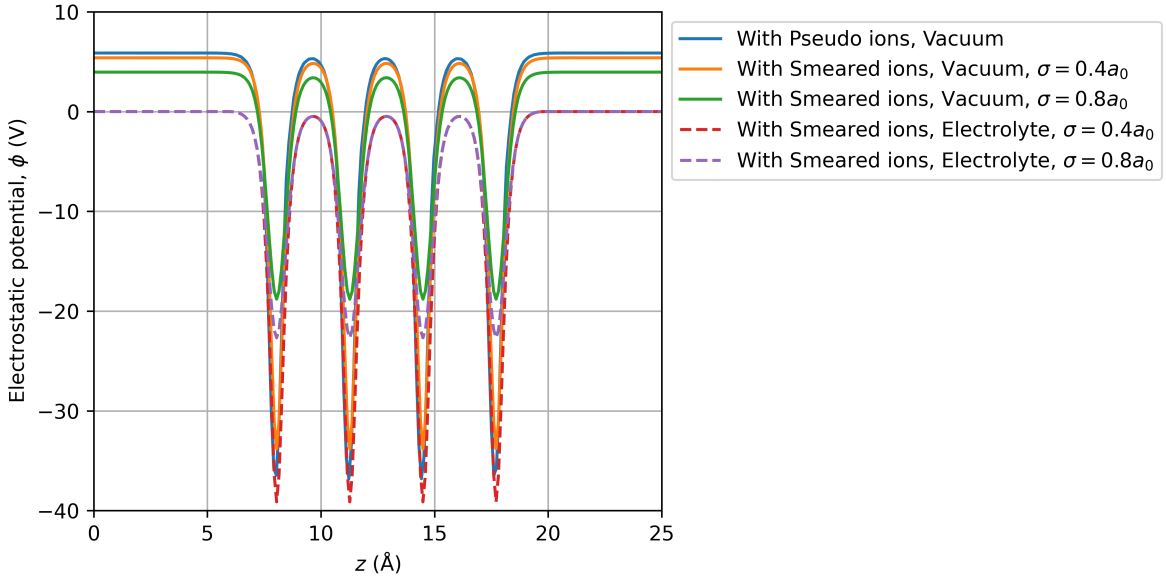

Fig. S7: Planar averaged electrostatic potential along the z-axis, shown for pseudo ions and for smeared ions, where the smearing width is indicated in the legend.

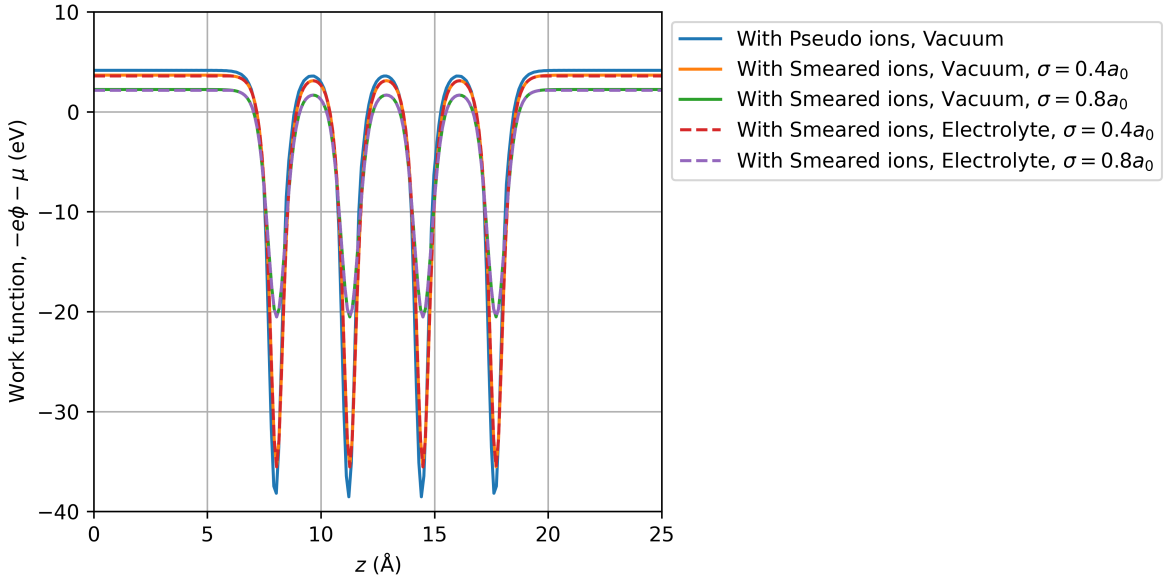

Fig. S8: Adjusted planar averaged electrostatic potential along the z-axis, shown for pseudo ions and for smeared ions, where the smearing width, σ, is indicated in the legend. The value e is the elementary charge, ϕ is the electrostatic potential and μ is the chemical potential of electrons (also known as the Fermi level). a_0 is the Bohr radius. In the vacuum region, the value indicated is equivalent to the work function.